



# Magnetic structures of the ternary stannide $U_2(Ni_{0.70}Pd_{0.30})_2Sn$

D. Laffargue<sup>a,b</sup>, F. Bourée<sup>b,\*</sup>, B. Chevalier<sup>a</sup>, T. Roisnel<sup>b</sup>, S. Bordère<sup>a</sup>

<sup>a</sup>Institut de Chimie de la Matière Condensée de Bordeaux, ICMCB-CNRS (UPR 9048), Université de Bordeaux I, Avenue du Dr A. Schweitzer, 33608 Pessac, France

<sup>b</sup>Laboratoire Léon Brillouin, CEA-CNRS, CEA/Saclay, 91191 Gif sur Yvette, France

## Abstract

The Néel temperature  $T_N$  in the tetragonal (P4/mbm space group) antiferromagnetic  $U_2(Ni_{1-x}Pd_x)_2Sn$  solid solution exhibits a minimum ( $T_N=12(1)$  K) at  $x\approx 0.30-0.35$ ; the end values being respectively equal to  $T_N=25$  K ( $x=0$ ) and  $T_N=42$  K ( $x=1$ ). In order to understand this  $T_N$  vs.  $x$  dependence, we have investigated the  $U_2(Ni_{0.70}Pd_{0.30})_2Sn$  stannide by neutron powder diffraction. This alloy exhibits two magnetic transitions, at  $T_N=11.5(5)$  K and  $T_{N'}=8.0(5)$  K. Between  $T_{N'}$  and  $T_N$ , the magnetic peaks are associated to  $\mathbf{k}=(0\ 0\ 1/2)$  propagation vector; below  $T_{N'}$ , two propagation vectors are present,  $\mathbf{k}=(0\ 0\ 1/2)$  and  $\mathbf{k}'=(1/2\ 1/2\ 1/2)$ , which are associated to different volumes of the sample. We discuss this complex magnetic behaviour, in connection with the  $U_2Ni_2Sn$  ( $\mathbf{k}=(0\ 0\ 1/2)$ ) and  $U_2Pd_2Sn$  ( $\mathbf{k}''=(0\ 0\ 0)$ ) magnetic structures. © 1998 Elsevier Science S.A.

**Keywords:** Ternary stannides; Neutron diffraction; Magnetic structures; Magnetic phase diagram

## 1. Introduction

Recently, the magnetic properties of the  $U_2(Ni_{1-x}Pd_x)_2Sn$  ternary stannides ( $0\leq x\leq 1$ ), crystallizing in the tetragonal ordered  $U_3Si_2$ -type structure (P4/mbm space group, with U in (4h), (Ni, Pd) in (4g) and Sn in (2a) Wyckoff positions) were investigated [1]. All the compositions order antiferromagnetically, showing an interesting behaviour of the Néel temperature  $T_N$ :  $T_N$  first decreases from 25 K ( $x=0$ ) to 12 K ( $x=0.30-0.35$ ) and then increases up to 42 K ( $x=1.0$ ). This  $T_N=f(x)$  dependence was reproduced on account of an anisotropic RKKY (Ruderman–Kittel–Kasuya–Yosida) model [1], the occurrence of a minimum in  $T_N(x)$  being associated to a change in magnetic structure, from the  $U_2Ni_2Sn$ ,  $\mathbf{k}=(0\ 0\ 1/2)$  collinear magnetic structure described in Ref. [2] to the  $U_2Pd_2Sn$ ,  $\mathbf{k}''=(0\ 0\ 0)$  non-collinear structure [3,4].

In order to prove this calculated magnetic phase, we performed neutron powder diffraction on the  $U_2(Ni_{1-x}Pd_x)_2Sn$  system. In this paper, we discuss pre-

liminary results concerning the  $U_2(Ni_{0.70}Pd_{0.30})_2Sn$  ternary stannide.

## 2. Experimental

The  $U_2(Ni_{0.70}Pd_{0.30})_2Sn$  sample was prepared by melting stoichiometric amounts of the constituent elements under argon atmosphere. The obtained alloy was then annealed for 1 month at 800°C under vacuum in a quartz crucible. Microprobe analysis and X-ray powder diffraction at  $T=300$  K confirmed that this annealed alloy is single phase and crystallizes in the tetragonal  $U_3Si_2$ -type structure, with  $a=7.379(2)$  Å and  $c=3.714(1)$  Å as unit-cell parameters.

Magnetization measurements were carried out in the 2–20 K temperature range using a Superconducting QUantum Interference Device (SQUID) magnetometer.

Neutron diffraction experiments have been performed at the Orphée reactor (Saclay, France), on the G4.1 two-axis diffractometer (800 cell PSD,  $\lambda=2.4265$  Å). Neutron data were analysed with the Rietveld-type FULLPROF program [5], with scattering neutron lengths from Ref. [6]:  $b_U=0.8417\times 10^{-12}$  cm,  $b_{Ni}=1.03\times 10^{-12}$  cm,  $b_{Pd}=0.591\times$

\*Corresponding author. Tel.: +33 1 69085449; fax: +33 1 69088261; e-mail: bouree@bali.saclay.cea.fr

$10^{-12}$  cm and  $b_{\text{Sn}}=0.6225 \times 10^{-12}$  cm. The  $\text{U}^{3+}$  magnetic form factor was calculated as  $\langle j_0 \rangle$ , with  $\langle j_0 \rangle$  values from Ref. [7].

### 3. Results

#### 3.1. Magnetization measurements

Fig. 1 shows the temperature dependence of the magnetization  $M$  of  $\text{U}_2(\text{Ni}_{0.70}\text{Pd}_{0.30})_2\text{Sn}$  below 20 K. Two features are observed in the derivative curve  $dM/dT=f(T)$  (inset of Fig. 1): a well-defined maximum occurring at  $T_N=12(1)$  K and a ‘shoulder’ occurring at  $T_{N'}=7(1)$  K. These results suggest the existence of two magnetic transitions for this stannide.

#### 3.2. Neutron powder diffraction

At  $T=16$  K  $>T_N$ , the neutron powder diffraction pattern of this stannide reveals reflections associated to nuclear scattering only: the  $\text{U}_2(\text{Ni}_{0.70}\text{Pd}_{0.30})_2\text{Sn}$  unit-cell parameters are then equal to  $a=7.3614(5)$  Å and  $c=3.7306(3)$  Å.

Neutron powder diffraction diagrams at low temperatures (Fig. 2) clearly show the existence of new Bragg peaks, connected to 3D antiferromagnetic ordering in  $\text{U}_2(\text{Ni}_{0.70}\text{Pd}_{0.30})_2\text{Sn}$ . The type of antiferromagnetic order is temperature dependent: if all the magnetic Bragg peaks at  $T=9.8$  K can be indexed with the help of a  $\mathbf{k}=(0\ 0\ 1/2)$  propagation vector, two propagation vectors are necessary at  $T=1.5$  K:  $\mathbf{k}=(0\ 0\ 1/2)$  and  $\mathbf{k}'=(1/2\ 1/2\ 1/2)$ . From thermal variation of  $(1\ 0\ 1/2)$ ,  $(1\ 1\ 1/2)$  and  $(2\ 1\ 1/2)$  (Fig. 3),  $(1/2\ 1/2\ 1/2)$  and  $(3/2\ 1/2\ 1/2)$  (Fig. 4) mag-

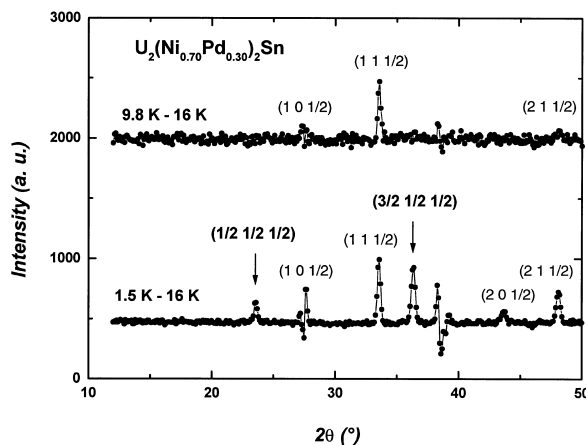


Fig. 2.  $\text{U}_2(\text{Ni}_{0.70}\text{Pd}_{0.30})_2\text{Sn}$  neutron powder diffraction ( $\lambda=2.4265$  Å) difference diagrams:  $T(T=16$  K  $>T_N$ ). Two diagrams are shown at, respectively,  $T=9.8$  K [ $T_{N'} < T < T_N$ ] and  $T=1.5$  K [ $T < T_{N'}$ ].

netic intensities, two magnetic transition temperatures are obtained:  $T_N=11.5(5)$  K and  $T_{N'}=8.0(5)$  K, in excellent agreement with the values obtained from magnetization measurements. Moreover, the  $\mathbf{k}=(0\ 0\ 1/2)$  magnetic structures below  $T_{N'}$  and between  $T_{N'}$  and  $T_N$  are different, as reflected by the differences in the magnetic  $(h\ k\ 1/2)$  intensity ratios in the intermediate and low temperature ranges (Fig. 3).

#### 3.2.1. Magnetic structure at $T=9.8$ K

The analysis was done with the help of magnetic group theory for  $P4/m\text{b}m$  space group,  $(4h)$  Wyckoff position and  $\mathbf{k}=(0\ 0\ 1/2)$  propagation vector [2]. In the intermediate temperature range ( $T_{N'} < T < T_N$ ), the best fit

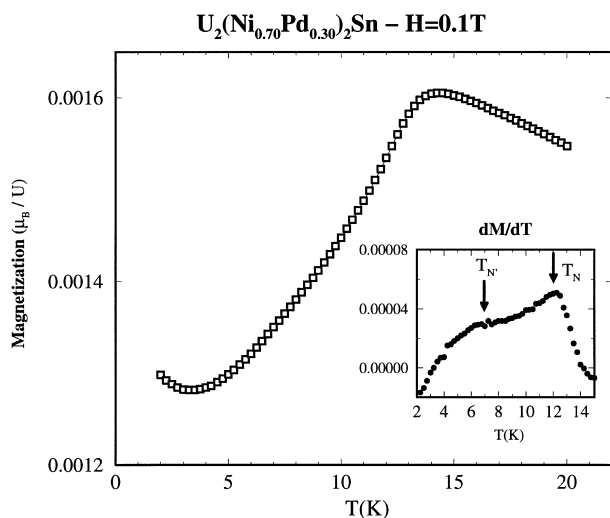


Fig. 1. Thermal variation of  $\text{U}_2(\text{Ni}_{0.70}\text{Pd}_{0.30})_2\text{Sn}$  magnetization (external field  $H=0.1$  T). The inset shows the derivative  $dM/dT$  ( $M$ , magnetization;  $T$ , temperature).

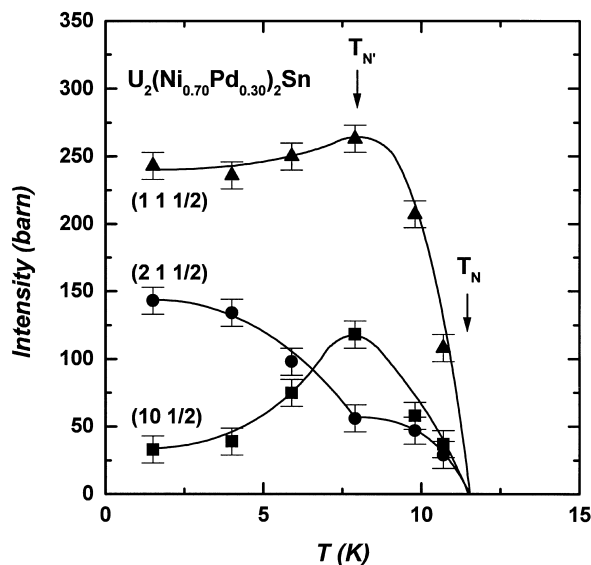


Fig. 3.  $\text{U}_2(\text{Ni}_{0.70}\text{Pd}_{0.30})_2\text{Sn}$ , thermal variation of  $(1\ 0\ 1/2)$ ,  $(1\ 1\ 1/2)$  and  $(2\ 1\ 1/2)$  magnetic intensities. These magnetic Bragg peaks are associated to  $\mathbf{k}=(0\ 0\ 1/2)$  wave vector.

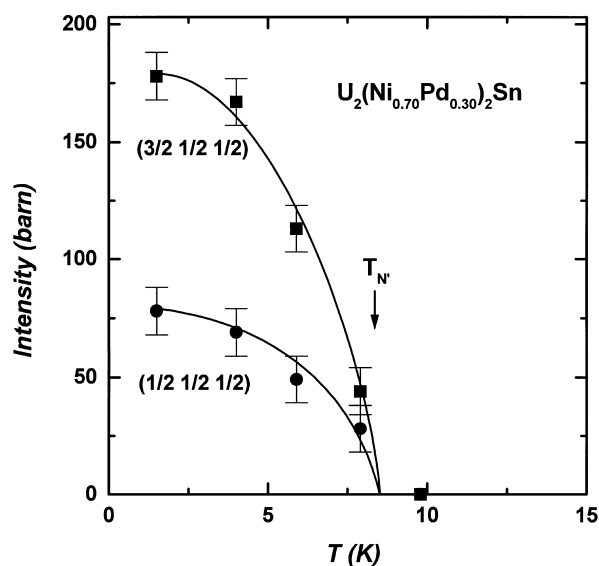


Fig. 4.  $U_2(Ni_{0.70}Pd_{0.30})_2Sn$ , thermal variation of  $(1/2\ 1/2\ 1/2)$  and  $(3/2\ 1/2\ 1/2)$  magnetic intensities. These magnetic Bragg peaks are associated to  $\mathbf{k}'=(1/2\ 1/2\ 1/2)$  wave vector.

between observed and calculated data is obtained for  $\Gamma_8$  irreducible representation (Fig. 5a), with  $M_U=0.55(5)\ \mu_B$  at  $T=9.8\ K$  (reliability factor  $R_M=9\%$ ).

### 3.2.2. Magnetic structure at $T=1.5\ K$

Contrary to what happens in the intermediate temperature range, the  $\mathbf{k}=(0\ 0\ 1/2)$  magnetic diagram at  $T=1.5\ K$  cannot be accounted for by a unique irreducible representation  $\Gamma_i$  ( $i=1-10$ ): two of them are now present,  $\Gamma_8$  and  $\Gamma_2$ . For both of these magnetic arrangements, the U-magnetic moments are parallel to the tetragonal c-axis:  $\Gamma_2$  magnetic structure is characterized by ferromagnetic (001) planes, with the '+-+-' stacking sequence along the c-axis (Fig. 5b).

From magnetic group theory applied to the  $P4/mmb$  space group, (4h) Wyckoff position and  $\mathbf{k}'=(1/2\ 1/2\ 1/2)$  propagation vector [8], as many as 10 irreducible representations  $\tau_j$  ( $j=1-10$ ) are obtained. In  $U_2(Ni_{0.70}Pd_{0.30})_2Sn$ , the  $\mathbf{k}'=(1/2\ 1/2\ 1/2)$  magnetic structure at  $T=1.5\ K$  is accounted for by  $\tau_{10}$ ; for this arrangement (magnetic unit cell  $2a \times 2a \times 2c$ ), the U-magnetic moments are also parallel to the c-axis (Fig. 5c).

Three different types of magnetic ordering are then

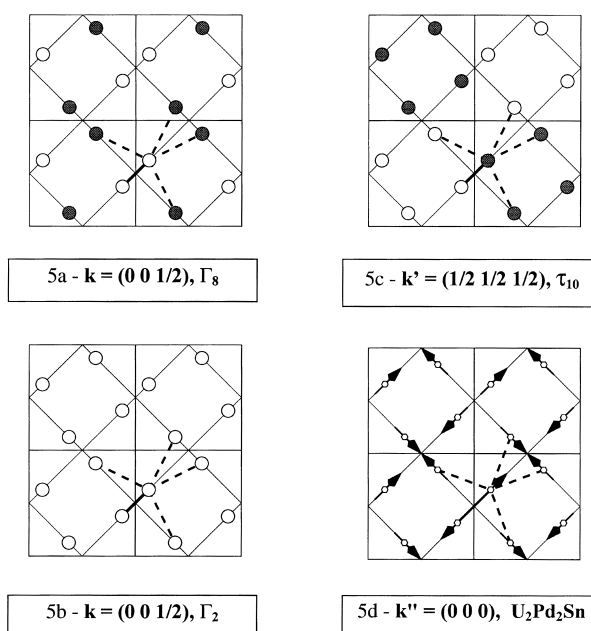


Fig. 5. (a)  $\mathbf{k}=(0\ 0\ 1/2)$ ,  $\Gamma_8$  magnetic structure; (b)  $\mathbf{k}=(0\ 0\ 1/2)$ ,  $\Gamma_2$  magnetic structure; (c)  $\mathbf{k}'=(1/2\ 1/2\ 1/2)$ ,  $\tau_{10}$  magnetic structure; (d)  $\mathbf{k}''=(0\ 0\ 0)$ ,  $U_2Pd_2Sn$  magnetic structure. For  $\mathbf{k}'=(1/2\ 1/2\ 1/2)$ , an a-, b- or c-translation implies a change in the sign of the U magnetic moment. For  $\mathbf{k}=(0\ 0\ 1/2)$ , only a c-translation changes this sign. Four crystalline unit-cells, i.e.  $2a \times 2a \times c$ , are shown in the figures. For all these magnetic structures, except  $U_2Pd_2Sn$  (d), the U magnetic moments are parallel to the tetragonal c-axis (open circles, spins 'up'; full circles, spins 'down'). The shortest  $d_{U-U}$  distances within (a,b)-plane are indicated either by continuous (one distance,  $d_{1U}$ ) or dashed lines (four distances,  $d_{4U}$ ).

observed at  $T=1.5\ K$  for U-magnetic moments. Two assumptions can be made (and neutron powder diffraction is not able to choose between these two): either ' $\mathbf{k}=(0\ 0\ 1/2)$ ,  $\Gamma_8$ ', ' $\mathbf{k}=(0\ 0\ 1/2)$ ,  $\Gamma_2$ ' and ' $\mathbf{k}'=(1/2\ 1/2\ 1/2)$ ,  $\tau_{10}$ ' are all associated to the whole volume of the sample, or each of these magnetic arrangements is associated to a partial volume in the sample. We selected the partial volume assumption, from the criterium of identical magnetic moment values for the four U atoms in the nuclear unit cell. The results of the neutron powder diffraction ( $T=1.5\ K$ ) magnetic data refinement are given in Table 1. At  $T=1.5\ K$ , the U-magnetic moment is equal to  $1.05(10)\ \mu_B/U$ , identical to the value obtained at the same temperature for  $x=0$  [2], and far below the ' $x=1$ ' value ( $2.20\ \mu_B/U$  [3]).

Table 1

$U_2(Ni_{0.70}Pd_{0.30})_2Sn$  magnetic structures at  $T=1.5\ K$ : propagation vector ( $\mathbf{k}$  or  $\mathbf{k}'$ ), magnetic structure type ( $\Gamma_i$  or  $\tau_j$ ), U magnetic moment and volume of the associated magnetic domain

Propagation vector	Magnetic structure	Magnetic moment ( $\mu_B$ )	Volume (%)	Reliability factor, $R_M$ (%)
$\mathbf{k}=(0\ 0\ 1/2)$	$\Gamma_8$	$M_U=1.05(10)$	30(5)	2.10
$\mathbf{k}=(0\ 0\ 1/2)$	$\Gamma_2$	$M_U=1.05(10)$	25(5)	5.05
$\mathbf{k}'=(1/2\ 1/2\ 1/2)$	$\tau_{10}$	$M_U=1.05(10)$	45(5)	9.35

These values are obtained from neutron powder diffraction FULLPROF [5] data refinement.

Table 2

$U_2(Ni_{1-x}Pd_x)_2Sn$  alloys, magnetic exchange interactions between nearest U neighbours, at distances  $d_{1U}$ ,  $d_{2U}$  and  $d_{4U}$  (the number of such neighbours is indicated by the digit in the index of  $d_{nU}$ ; neighbours within (a,b)-plane, at distances  $d_{1U}$  and  $d_{4U}$ , are shown in Fig. 5)

	Propagation vector	Magnetic structure	$d_{1U}$ ( $\perp$ c-axis)	$d_{2U}=c$ ( $\parallel$ c-axis)	$d_{4U}$ ( $\perp$ c-axis)
$U_2Ni_2Sn$	$\mathbf{k}=(0\ 0\ 1/2)$	$\Gamma_{10}$	F	AF	AF
$U_2(Ni_{0.7}Pd_{0.3})_2Sn$	$\mathbf{k}=(0\ 0\ 1/2)$	$\Gamma_8$	F	AF	AF
	$\mathbf{k}=(0\ 0\ 1/2)$	$\Gamma_2$	F	AF	F
	$\mathbf{k}'=(1/2\ 1/2\ 1/2)$	$\tau_{10}$	AF	AF	2F & 2AF
$U_2Pd_2Sn$	$\mathbf{k}''=(0\ 0\ 0)$	$\Gamma_8'$	AF	F	—

F, ferromagnetic; AF, antiferromagnetic.

#### 4. Discussion

Contrary to the end compounds,  $U_2Ni_2Sn$  and  $U_2Pd_2Sn$ , where only one magnetic transition occurs, two magnetic transition temperatures are obtained for  $U_2(Ni_{0.70}Pd_{0.30})_2Sn$ :  $T_N=11.5(5)$  K and  $T_{N'}=8.0(5)$  K.

Let us now compare the magnetic structures in the  $U_2(Ni_{1-x}Pd_x)_2Sn$  series: they are known, up to now, for  $x=0$  [2],  $x=1$  [3,4] (Fig. 5d) and  $x=0.30$  (this work). All are antiferromagnetic, but all are different (Table 2, Fig. 5). Let us just recall that the  $U_2Ni_2Sn$  magnetic structure [ $\mathbf{k}=(0\ 0\ 1/2)$ ,  $\Gamma_{10}$ ] is similar to the [ $\mathbf{k}=(0\ 0\ 1/2)$ ,  $\Gamma_8$ ] structure (Fig. 5a), except for the direction of the U-moments, which are either perpendicular ( $U_2Ni_2Sn$ ) or parallel ( $U_2(Ni_{0.70}Pd_{0.30})_2Sn$ ) to the tetragonal c-axis. At the other end of the series (i.e. for  $x=1$ ,  $U_2Pd_2Sn$ ), the magnetic structure is associated to [ $\mathbf{k}''=(0\ 0\ 0)$ ,  $\Gamma_8'$ ] [9] and depicted in Fig. 5d. So, for  $U_2Ni_2Sn$  and  $U_2Pd_2Sn$ , the magnetic interactions between nearest U neighbours (at  $d_{1U}$  and  $d_{2U}$  distances, Table 2) are respectively F, AF ( $U_2Ni_2Sn$ ) and AF, F ( $U_2Pd_2Sn$ ), which means an inversion of the sign of interactions ( $F \leftrightarrow AF$ ) when going from  $x=0$ ,  $U_2Ni_2Sn$  to  $x=1$ ,  $U_2Pd_2Sn$ . Some equilibrium between these competing magnetic interactions is then to be found at intermediate  $x$  values. For  $U_2(Ni_{1-x}Pd_x)_2Sn$ ,  $x=0.30$ , the 'equilibrium' at low temperature ( $T < T_{N'}$ ) is obtained via different volumes of the same sample, associated to different magnetic structures. For these magnetic structures, the magnetic interactions between U nearest neighbours are either F, AF or AF, AF (Table 2).

The  $U_2(Ni_{1-x}Pd_x)_2Sn$  magnetic ground state and  $T_N(x)$  value have been accounted for in the frame of an anisotropic RKKY model [1]: for this calculation of magnetic RKKY exchange interaction, not only three (at  $d_{1U}$  and  $d_{2U}$  distances) or seven (at  $d_{1U}$ ,  $d_{2U}$  and  $d_{4U}$  distances) U

neighbours were considered, but about 300, which are included in a sphere of 15 Å radius. It was then shown that the minimum of  $T_N(x)$  observed at  $x \approx 0.30-0.35$  in the  $U_2(Ni_{1-x}Pd_x)_2Sn$  solid solution was associated to a change of magnetic structure type, from  $U_2Ni_2Sn$  to  $U_2Pd_2Sn$ -type magnetic structure. Let us note that the [ $\mathbf{k}=(0\ 0\ 1/2)$ ,  $\Gamma_{10}$ ] ( $U_2Ni_2Sn$ ) and [ $\mathbf{k}=(0\ 0\ 1/2)$ ,  $\Gamma_8$ ] ( $U_2(Ni_{0.70}Pd_{0.30})_2Sn$ ) magnetic structures, as they are similar except for the direction of the U magnetic moments, are associated to the same magnetic exchange energy. An extension of this anisotropic RKKY model to the [ $\mathbf{k}'=(1/2\ 1/2\ 1/2)$ ] magnetic states, which have not been taken into account in Ref. [1], has to be done now, together with neutron powder diffraction on other compounds in the series ( $0.30 < x < 1$ ), in order to get a deeper insight in the complex  $U_2(Ni_{1-x}Pd_x)_2Sn$  magnetic phase diagram.

#### References

- [1] S. Bordère, S. Buzdin, B. Chevalier, D. Laffargue, J. Etourneau, J. Magn. Magn. Mater. 175 (1997) 263.
- [2] F. Bourée, B. Chevalier, L. Fournès, F. Mirambet, T. Roisnel, V.H. Tran, Z. Zolnieriek, J. Magn. Magn. Mater. 138 (1994) 307.
- [3] D. Laffargue, F. Bourée, B. Chevalier, T. Roisnel, P. Gravereau, J. Etourneau, J. Magn. Magn. Mater. 170 (1997) 155.
- [4] A. Purwanto, R.A. Robinson, L. Havela, V. Sechovsky, P. Svoboda, H. Nakotte, K. Prokes, F.R. de Boer, A. Seret, J.M. Winand, J. Rebizant, J.C. Spirlet, Phys. Rev. B 50 (1994) 6792.
- [5] J. Rodriguez-Carvajal, Physica B 192 (1993) 55.
- [6] V.F. Sears, Neutron News 3(3) (1992) 26.
- [7] A.J. Freeman, J.P. Desclaux, J. Magn. Magn. Mater. 12 (1979) 11.
- [8] D. Laffargue, Thèse, Université de Bordeaux I (France), no. 1734, 1997.
- [9] F. Bourée, B. Chevalier, D. Laffargue, T. Roisnel, in: Workshop on Application of Symmetry Analysis to Diffraction Investigations, Krakow, Poland, Extended Abstracts, 1996, pp. 9–14.